ELSEVIER

Journal of Nuclear Materials 313–316 (2003) 1304–1308

journal of nuclear materials

www.elsevier.com/locate/jnucmat

Plasma boundary considerations for the national compact stellarator experiment

P. Mioduszewski [a,*], A. Grossman [b], M. Fenstermacher [c], A. Koniges [c], L. Owen [a], T. Rognlien [c], M. Umansky [c]

[a] *Oak Ridge National Laboratory, P.O. Box 2009, Oak Ridge, TN 37831, USA*
[b] *University of California, San Diego, CA 92093, USA*
[c] *Lawrence Livermore National Laboratory, Livermore, CA 94551, USA*

Abstract

The national compact stellarator experiment (NCSX) [EPS 2001, Madeira, Portugal, 18–22 June 2001] is a new fusion project located at Princeton Plasma Physics Laboratory, Princeton, NJ. Plasma boundary control in stellarators has been shown to be very effective in improving plasma performance [EPS 2001, Madeira, Portugal, 18–22 June 2001] and, accordingly, will be an important element from the very beginning of the NCSX design. Plasma-facing components will be developed systematically according to our understanding of the NCSX boundary, with the eventual goal to develop a divertor with all the benefits for impurity and neutrals control. Neutrals calculations have been started to investigate the effect of neutrals penetration at various cross-sections.

PACS: 52.40.Hf
Keywords: Plasma boundary; Divertors; Compact stellarators; Stochastic fields

1. Introduction

The national compact stellarator experiment (NCSX) is a new fusion project of the US fusion program, designed with the goal to develop a more compact fusion reactor configuration which is intrinsically capable of steady state operation and avoidance of disruption problems [1]. The design incorporates tokamak and Stellarator features for optimum confinement and stability. The main machine parameters are: $R = 1.4$ m, $\langle a \rangle = 0.32$ m, three field periods, $B \leqslant 2$ T, $P_{\mathrm{NBI}} = 6$ MW, $P_{\mathrm{rf}} = 6$ MW. Approximately 75% of the rotational transform is provided by external coils and the rest by the bootstrap current.

2. Development of plasma-facing components

It has been shown that plasma boundary control is a key element in improving plasma performance in stellarators [2,3], as it has been for tokamaks. Accordingly, the NCSX program incorporates a strong plasma boundary component from the very start of the design. The plasma edge in NCSX is 3-dimensional and stochastic and developing optimal plasma-facing components (PFCs) will take some iterations between modeling and experiment. The PFCs will have complicated shapes according to the 3-D plasma topology. A top view of the plasma contour with the modular coils is shown in Fig. 1. Since our understanding of the plasma boundary is limited at the beginning of operation, we will take a phased approach to the development of the PFCs.

In a stellarator, the plasma boundary can be very complex, with islands and ergodic regions with short connection lengths which can themselves interact locally with the walls. Therefore, for initial operation, limiter operation may be more easily controllable, although it

* Corresponding author. Tel.: +1-865 574 2715; fax: +1-865 574 1191.
E-mail address: mioduszewspk@ornl.gov (P. Mioduszewski).

0022-3115/03/$ - see front matter
PII: S0022-3115(02)01505-2

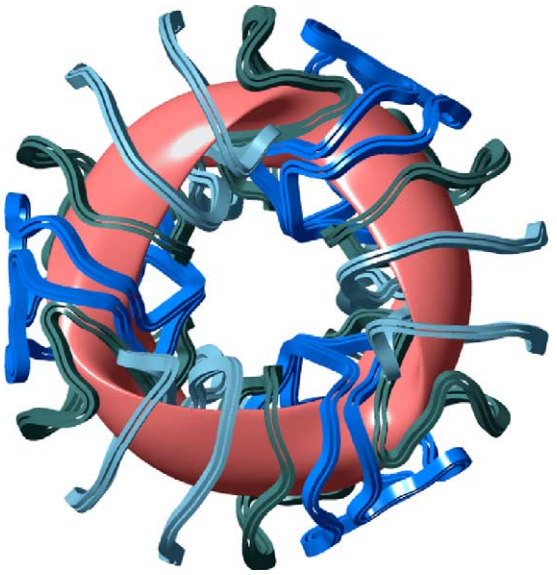

Fig. 1. Plasma contour and modular coils of the NCSX.

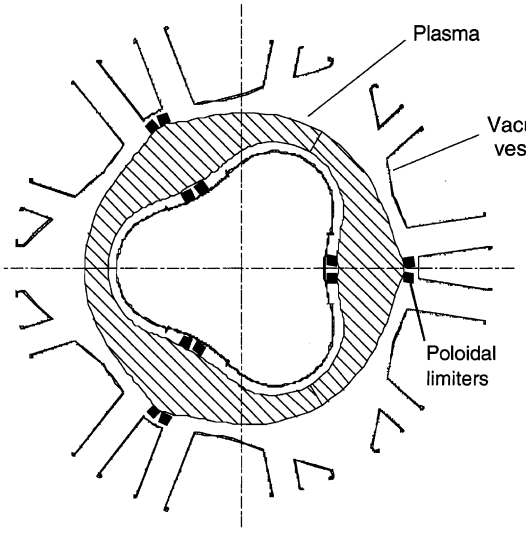

Fig. 2. First generation of PFCs: poloidal limiters at the $\phi = 60°$ location.

will likely not be optimal for plasma performance. The first generation of PFCs will simply consist of three poloidal limiters (one for each field-period at $\phi = 60°$), depicted in Fig. 2, which will be sufficient to protect the walls and perform Ohmic operation.

The second generation of PFCs will have to be installed simultaneously with auxiliary heating. It will consist of graphite wall armor on the inboard side of the vacuum vessel, as is schematically shown in Fig. 3. This armor will extend toroidally around; the exact configuration at $\phi = 60°, \ldots$ is still under discussion. The configuration should be flexible enough to explore various plasma configurations and their interactions with the wall. It will also provide the first opportunity to study boundary configurations with finite plasma pressure. In this configuration it should be possible to explore plasmas of various size as well as limiter or separatrix configurations.

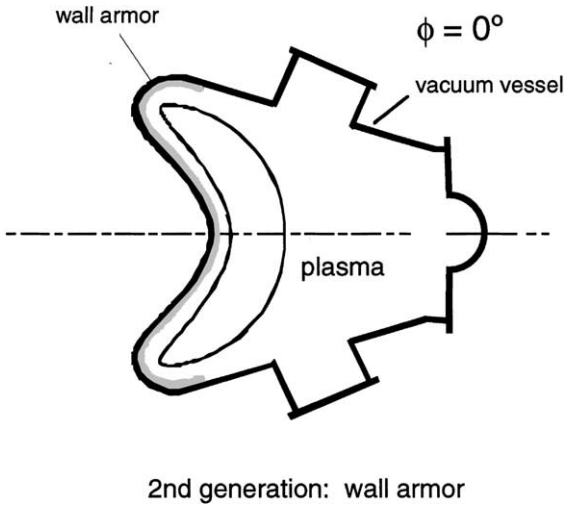

Fig. 3. Second generation of PFCs: toroidal inboard wall armor.

3. Magnetic topology outside the last closed magnetic surface

Based on recent results of W7-AS [2] divertor operation can make a major difference in plasma performance such as increasing the energy confinement time and reducing the particle and impurity confinement time, to name only two of the observed improvements. We assume that operation with the second generation of PFCs (Fig. 3) will provide us with the database necessary for a full divertor design.

In our computational studies, we have made extensive use of a code originally developed for the design of the divertor of the W7-X stellarator, magnetic field solver for finite beta equilibria (MFBE), which is a new magnetic topology code developed by Strumberger [4], for magnetic configurations which have finite plasma pressure. Prior calculations for the boundary of stellarators used only vacuum magnetic fields outside the last closed magnetic surface (LCMS). In addition to these vacuum fields, MFBE calculates all magnetic fields of finite-beta, free boundary equilibria with plasma currents on a grid whose nodes may be arbitrarily close to the plasma boundary. Unlike other stellarators, the

NCSX configuration has a bootstrap current comparable to a tokamak with the same iota, having an external transform fraction of about 75% and the rest by bootstrap current, which will contribute to the structure of the magnetic boundary.

For the NCSX boundary studies, the VMEC code is used to determine free boundary finite beta equilibria [5]. The upgraded VMEC2000 code is an energy minimizing equilibrium code which assumes nested flux surfaces and therefore cannot be used to study islands and stochastic regions inside the LCMS. Coupling of the VMEC2000 and MFBE codes allows the LCMS to be found by an iteration procedure.

Stellarators are generally lacking the ordered magnetic field line structure with nested surfaces found in the scrape-off layer of axisymmetric devices. For the M45 coil set of NCSX, the field lines do not form nested surfaces outside the LCMS, but make many toroidal revolutions close to it. This is shown in Fig. 4, which depicts Poincaré plots for planes with the toroidal angles of 0°, 30°, 60° and 90°.

The Poincaré plots in Fig. 4 are generated by following 10 field-lines each for 20 toroidal revolutions, launched from the inside midplane (red) and the outside midplane (green) respectively; the plots represent the full-current, full-beta case. Typical Kolmogorov lengths L_k for field-lines shown in Fig. 4 are in the order of 30–50 m, while the field-lines were followed for 20 revolutions, corresponding to 176 m. After 20 revolutions, about 80% of the field lines stay within a band of 2.5 cm outside the LCMS, so we assume that 80% of the field lines have connection lengths $L_c \geqslant 176$ m. This means that L_k is smaller than L_c, which means the field-lines are stochastic, but since we do not have $L_k \ll L_c$ the stochasticity is moderate. In conclusion, a large fraction of the field lines has sufficiently long connection lengths for divertor operation.

The second boundary characteristic, important for divertor operation, is the flux expansion in the divertor region. The Poincaré plot in Fig. 4 shows for the $\phi = 0°, \ldots$ cross-section a flux expansion of 5–10 between the midplane and the top and bottom of the bean shape.

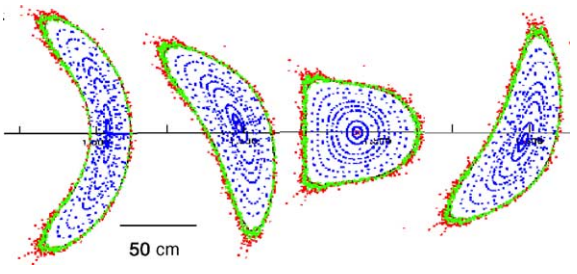

Fig. 4. Poincaré plots for the toroidal angles 0°, 30°, 60° and 90°; green field-lines launched on outer midplane (between 0 and 1 cm), red field-lines lauched on inner mid-plane.

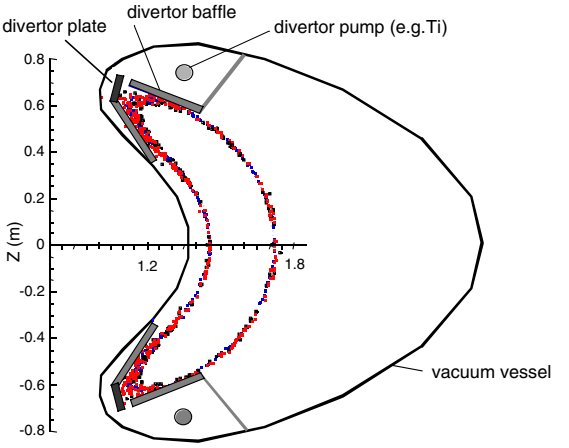

Fig. 5. Divertor configuration for NCSX with divertor plates, baffles and pumping option.

This looks very promising for manageable heat loads during divertor operation. A possible future divertor configuration with divertor plates, baffles, and pumps is shown in Fig. 5.

4. Heat flux peaking factors on the wall

Since the power loads on the wall depend largely on the specific design of the PFC configuration, we calculate here more generally typical peaking factors that can be expected from the characteristic stripes resulting from the plasma contacting the wall. As an example, we have chosen the $\phi = 60°, \ldots$ cross-section by moving the wall as close as 2 cm to the plasma to investigate the resulting peaking factors. Similar calculations will be done for the loads on the actual PFCs.

We have used field-line tracing to estimate the power loading on the wall surfaces. Here we describe the calculation of the relative distribution of intersecting field lines on the wall versus toroidal and poloidal angles. The data for the wall intersections are taken from the field-line tracing calculations using the Gourdon code following the work of Strumberger and Kisslinger [6,7].

The wall for these calculations is taken as a surface that is nearly conformal to the VMEC LCMS, but then shifted outward in major radius, such that the minimum gap on the inner wall is 2 cm, while on the outer wall, the gap is ~10 cm. This way, virtually all of the field-line intersections occur on the inside. The field-lines are then started at the LCMS and diffuse in the perpendicular direction with a diffusion coefficient of 1° m^2/s to simulate anomalous cross-field heat diffusion. In order to estimate the heat flux to the wall, we have produced a numerical distribution function of the field line intersections. The intersections with the wall are then binned

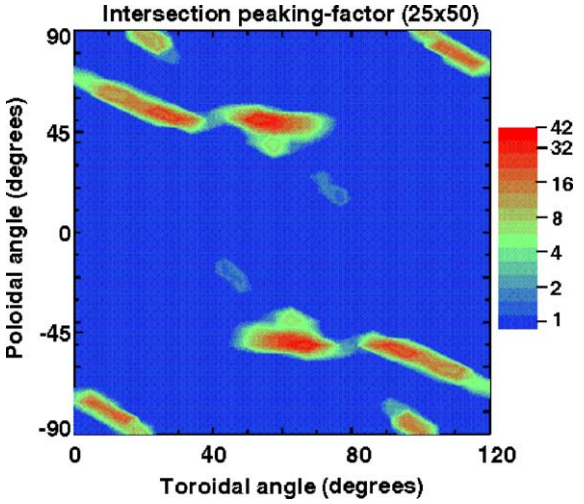

Fig. 6. Density of field-line distribution on the wall, normalized to uniform distribution showing a maximum peaking factor of 42.

on a uniform 2D mesh in (ϕ, θ) space using linear interpolation. The toroidal angle ϕ has its origin at the center of the bean cross-section, and the poloidal angle θ has the origin at the inner midplane of the cross-section. The result is shown in Fig. 6 where we have normalized the distribution such that it represents the increase over a uniform distribution of field-line intersections. The dark blue background corresponds to any value of the peaking factor less than unity.

This procedure provides a first estimate of typical peaking factors on the wall and predicts a maximum peaking factor of about 42, such that the maximum power load, $S_{\max}$, would be given by $S_{\max} = 42P_{\text{wall}}/A$, where P_{wall} is the power to the wall and A is the first-wall area, which is approximately 40 m^2. So, for a power flux of e.g. 6 MW to the wall, the peak power flux would be $\sim$6 MW/m^2.

5. Neutrals transport calculations

The primary objective of the neutrals studies reported here is to examine neutrals penetration at various plasma cross-sections. Effects of the 3-D geometry are determined with calculations in toroidally axisymmetric geometry for several poloidal cuts combined with a toroidal midplane cut. Particular attention is focused on neutral penetration of the radially thin region near $(\phi) = 0°, \ldots$ Background plasma parameters depend only upon the radial coordinate and are based on the W7-AS experimental database [8]. The scrape-off layer (SOL) grid surfaces are taken to be closed and approximately conformal to the LCMS. Density and temperature profiles are parabolic with central values of 6×10^{13} cm^{-3} and 1.5 keV, respectively. The assumed total recycling source is 3.75×10^{22} s^{-1}, based on 20 ms particle confinement time and a factor of 5 flux amplification. The ion temperatures and species fractions are based upon the average ion impact energy assuming a 3-kT_e sheath.

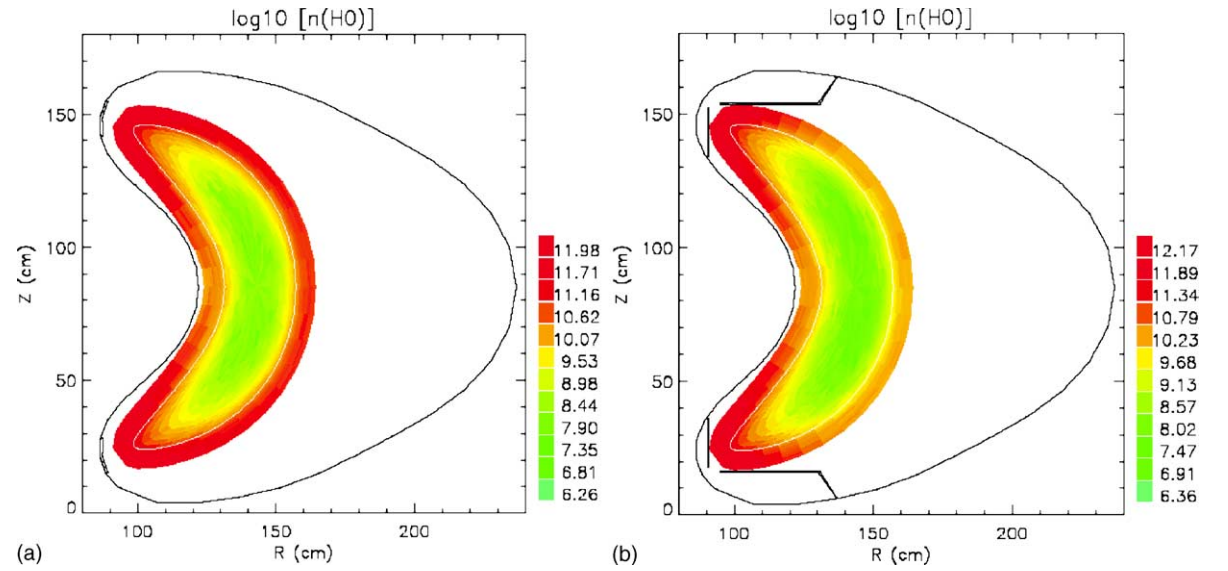

Fig. 7. (a) Neutrals distribution in $_{10}$log particles/cm^3 with inner graphite wall and recycling locations at $z = 20$ and 150 cm. (b) Neutrals distribution in $_{10}$log particles/cm^3 with divertor plates and baffles reduces the neutral density by a factor of 5 in the midplane.

Contour plots of the distributions of atomic neutral densities, calculated with the DEGAS code [9], are shown in Fig. 7(a) and (b) for the $\phi = 0°, \ldots$ cross-sections. The density contours are given in neutral particles per cm^3, where the particle number is given as the 10-based logarithm. Fig. 7(a) corresponds to the second generation of PFCs, i.e. the graphite wall armor. The recycling locations are indicated at the top and bottom inboard areas. This is where most of the recycling should occur according to the Poincaré plot in Fig. 4. We see that in our model the neutrals experience a large decrease in the SOL already. From the LCMS to the confinement region, the neutral density decays by about four orders of magnitude. In Fig. 7(b), which corresponds to our third generation of PFCs, we have added baffles to the divertor regions and the particles recycle at the vertical plate. Here again, we see that the neutral density in the core drops by several orders of magnitude. We also find that the geometrical baffling of the neutrals in the divertor region can reduce the midplane pressure by a factor of ≈ 5.

To evaluate the toroidal neutrals transport, simulations are also performed for the equatorial midplane geometry in which the recycling locations are the vacuum vessel wall at $\phi = 0°, \ldots$ and $60°, \ldots$ in the outboard midplane. The results indicate that with the plasma parameters used here, the neutral atomic density drops by a factor of 10 within a toroidal distance of $1/2$ field period. If the recycling location is $\phi = 60°, \ldots$ the closer proximity of the wall and strongly ionizing SOL leads to a factor of 40 decrease in $n(\mathrm{H}°)$ at the same toroidal distance from the source.

6. Summary

Results from W7-AS and other stellarators have shown that plasma boundary control is an important tool for performance improvement of stellarators, just as it has been in the past two decades for tokamaks. The design of the new compact stellarator NCSX at Princeton Plasma Physics Laboratory will include boundary control techniques, which will eventually result in the implementation of a divertor. While the plasma boundary outside the LCMS does not have closed nested flux surfaces or distinct islands, the field-lines stay close to the LCMS for lengths of up to ~ 180 m and there is substantial flux expansion in the top and bottom of the bean cross-section (factor 5–10). Therefore, in spite of the stochastic nature of the boundary, the implementation of a divertor at a later phase of the experiment looks promising.

Acknowledgement

This work was supported by the U.S. Department of Energy under Contract No. DE-AC05-00OR-22725, DE-FG03-95ER54394, and W-7405-ENG-48.

References

[1] M.C. Zarnstorff et al., EPS 2001, Madeira, Portugal, 18–22 June 2001.
[2] P. Grigull et al., EPS 2001, Madeira, Portugal, 18–22 June 2001.
[3] S. Masuzaki et al., J. Nucl. Mater. 290–293 (2001) 12.
[4] E. Strumberger, Nucl. Fusion 37 (1997) 19.
[5] S.P. Hirshman et al., Comput. Phys. Commun. 43 (1986) 143.
[6] E. Strumberger et al., Proceedings of the 20th EPS Conference on Controlled Fusion and Plasma Physics, Lisboa, vol. 17C, Part II, 1993, p. 791.
[7] J. Kisslinger et al., Proceedings of the 21st EPS Conference on Controlled Fusion and Plasma Physics, Montpellier, vol. 18B, Part II, 1994, p. 368.
[8] K. McCormick et al., Proceedings of the 12th International Stellarator Conference, Madison, 1999.
[9] D. Heifetz et al., J. Comp. Phys. 46 (1982) 309.